

000 001 002 003 004 005 006 007 008 009 010 011 012 013 014 015 016 017 018 019 020 021 022 023 024 025 026 027 028 029 030 031 032 033 034 035 036 037 038 039 040 041 042 043 044 045 046 047 048 049 050 051 052 053 TEMPERATURE AS A META-POLICY: ADAPTIVE TEM- PERATURE IN LLM REINFORCEMENT LEARNING

Anonymous authors

Paper under double-blind review

ABSTRACT

Temperature is a crucial hyperparameter in large language models (LLMs), controlling the trade-off between exploration and exploitation during text generation. High temperatures encourage diverse but noisy outputs, while low temperatures produce focused outputs but may cause premature convergence. Yet static or heuristic temperature schedules fail to adapt to the dynamic demands of reinforcement learning (RL) throughout training, often limiting policy improvement. We propose Temperature Adaptive Meta Policy Optimization (TAMPO), a new framework that recasts temperature control as a learnable meta-policy. TAMPO operates through a hierarchical two-loop process. In the inner loop, the LLM policy is updated (*e.g.*, using GRPO) with trajectories sampled at the temperature selected by the meta-policy. In the outer loop, meta-policy updates the distribution over candidate temperatures by rewarding those that maximize the likelihood of high-advantage trajectories. This trajectory-guided, reward-driven mechanism enables online adaptation without additional rollouts, directly aligning exploration with policy improvement. On five mathematical reasoning benchmarks, TAMPO outperforms baselines using fixed or heuristic temperatures, establishing temperature as an effective learnable meta-policy for adaptive exploration in LLM reinforcement learning.

1 INTRODUCTION

Reinforcement learning (RL) has become a promising paradigm for aligning large language models (LLMs) with human preferences and task-specific objectives (Ziegler et al., 2019; Ouyang et al., 2022; Bai et al., 2022; Chen et al., 2025). Traditional RLHF approaches often rely on PPO-based RL-based post-training, which requires a learned value network and incurs significant computational overhead. Recent critic-free algorithms, such as GRPO (Shao et al., 2024; Guo et al., 2025) and REINFORCE++ (Hu et al., 2025), demonstrate that large-scale LLM reinforcement learning can be both scalable and stable, bypassing the need for value networks while maintaining performance.

One of central challenges in RL remains the exploration–exploitation trade-off (Sutton et al., 1998; Kaelbling et al., 1996). For LLMs, sampling temperature serves as a direct and interpretable control knob: higher temperature produces a more uniform (random) distribution, encouraging diverse but potentially noisy generations, while lower temperature concentrates probability mass, favoring precision but at the risk of missing promising alternatives. Existing approaches, however, treat temperature as fixed or manually tuned, ignoring feedback from the learning process. Popular critic-free RL algorithms (*e.g.*, GRPO) (Shao et al., 2024; Guo et al., 2025; Hu et al., 2025; Yu et al., 2025) generate multiple rollouts at a given temperature to estimate trajectory advantages and policy gradients, but never adapt temperature based on trajectory outcomes.

We argue that temperature should be treated as a decision variable, not a fixed hyperparameter for LLM RL. Unlike entropy regularization coefficients or KL penalties, which influence exploration (Guo et al., 2025; Shen, 2025), temperature directly modulates the sampling distribution over text outputs in a simple, transparent manner. This motivates our work on principled, trajectory-guided temperature adaptation for effective LLM policy learning.

In this work, we introduce Temperature Adaptive Meta Policy Optimization (TAMPO), a meta-learning framework that jointly optimizes the LLM policy, and a meta-policy over temperatures. Figure 1 shows the overall framework, which operates through a hierarchical two-loop process.

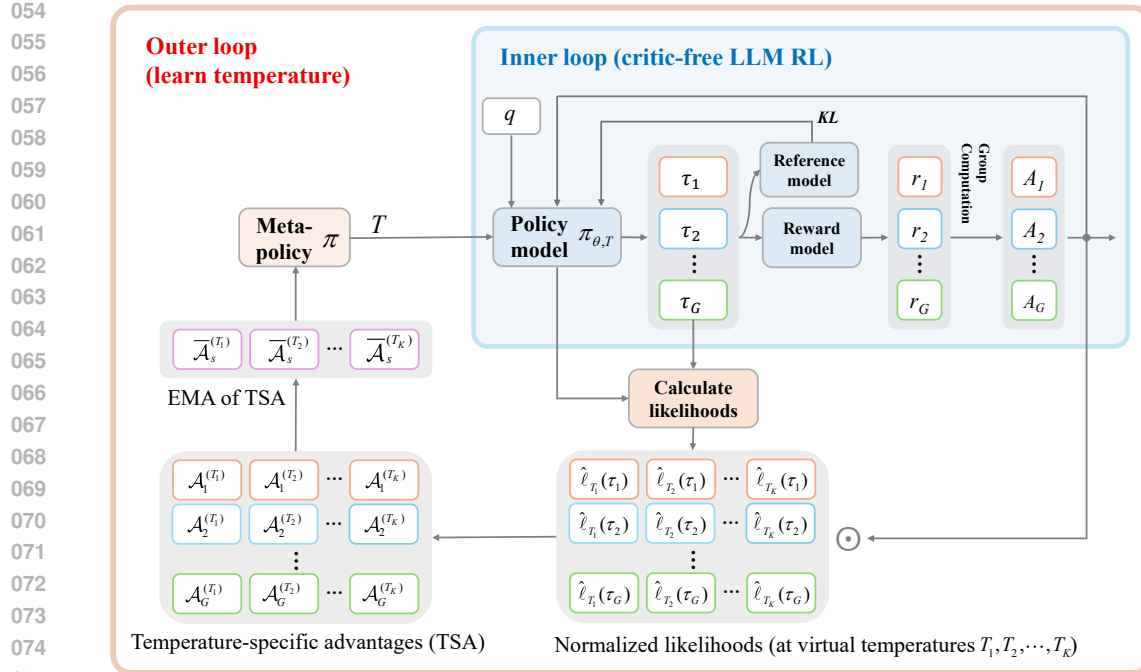


Figure 1: Overview of Temperature Adaptive Meta Policy Optimization (TAMPO). The framework operates through a hierarchical two-loop process. In the **inner loop**, the LLM policy is optimized with critic-free RL (e.g., GRPO) using rollouts sampled at the temperature chosen by the meta-policy. In the **outer loop**, the meta-policy is updated by evaluating trajectory likelihoods under virtual temperatures, deriving temperature-specific advantages ($A_i^{(T_k)} = \hat{\ell}_{T_k}(\tau_i) \cdot A_i$ for trajectory τ_i w.r.t. virtual temperature T_k), and reinforcing those that yield high-advantage rollouts (see §3). This design establishes temperature as a learnable meta-policy, enabling online adaptation and effective optimization of LLM policy without extra rollouts.

In the inner loop, the LLM policy model $\pi_{\theta,T}$ is optimized using critic-free RL (e.g., GRPO) at a sampled temperature T . In the outer loop, a meta-policy π is obtained based on temperature-specific advantages by reusing the inner loop rollouts, reinforcing temperatures that are more likely to generate trajectories with high advantages.

Intuitively, the temperatures that facilitate discovering rewarding outputs are reinforced, while the ineffective ones are suppressed, allowing the learned temperature to dynamically align with policy improvement.

We summarize our main contributions as follows:

- We formulate temperature as a learnable meta-policy in LLM RL, reframing temperature selection as a policy optimization problem to enhance adaptive, reward-driven exploration.
- We propose TAMPO, a hierarchical framework that jointly updates the LLM policy and a meta-policy over temperatures, rewarding those that prompt high-advantage rollouts.
- On five challenging mathematical reasoning benchmarks, TAMPO achieves better performance than baselines using fixed or heuristic temperatures, demonstrating the effectiveness of our trajectory-guided adaptive temperature control in LLM reinforcement learning.

TAMPO provides a principled, end-to-end, feedback-driven mechanism to dynamically balance exploration and exploitation, eliminating manual temperature sweeps, and improving the effectiveness of RL-based post-training.

108

2 RELATED WORK

110 **Critic-Free RL Methods.** Critic-free RL algorithms, such as REINFORCE Leave-One-Out
 111 (RLOO) (Kool et al., 2019), GRPO (Shao et al., 2024; Guo et al., 2025), DAPO (Yu et al., 2025), and
 112 REINFORCE++ (Hu et al., 2025) eliminate the need for learning value networks (critics), making
 113 them more efficient and scalable for LLM RL-based post-training. However, these approaches still
 114 mainly rely on fixed sampling temperatures, which may lead to under-exploration when the training
 115 temperature is too low, or wasted computation and noisy samples when too high. Our method
 116 complements these algorithms by learning a meta-policy over temperatures, which adapts sampling
 117 based on trajectory outcomes to better guide LLM policy optimization.

118 **Exploration–Exploitation in RL.** The exploration–exploitation dilemma is a fundamental chal-
 119 lenge in RL, where agents must balance between exploring new actions to discover potentially bet-
 120 ter strategies and exploiting known actions to maximize immediate rewards (Wang et al., 2025).
 121 Traditional methods, such as ϵ -greedy, [temperature annealing](#), and upper confidence bounds (UCB),
 122 employ fixed or heuristic schedules to manage this balance (Wikipedia contributors, 2025)(Sutton
 123 et al., 1998). Typically, ϵ -greedy linearly or exponentially decays ϵ over time, temperature anneal-
 124 ing gradually lowers the sampling temperature to reduce exploration, and UCB adaptively selects
 125 actions based on upper confidence bounds that balance estimated value and uncertainty. In RL for
 126 LLMs, maintaining exploration is crucial to avoid premature convergence to suboptimal reason-
 127 ing paths. Nucleus sampling (Holtzman et al., 2019) provides one practical strategy by restricting
 128 sampling to the smallest set of tokens whose cumulative probability exceeds a threshold p , thereby
 129 adaptively balancing diversity and reliability in generation, where p is in general fixed (e.g., 0.95).
 130 Entropy regularization is widely adopted to promote diverse outputs by encouraging higher-entropy
 131 policies (Guo et al., 2025; Shen, 2025). [Sethi et al.](#)(Sethi et al., 2025) view policy optimization as a
 132 [continuous-time dynamical system](#) and gradually decay the entropy regularization weight (typically
 133 as $1/t$). Shen (Shen, 2025) constrains entropy within a pre-defined range. However, the optimal
 134 entropy level during training remains unclear.

135 Beyond entropy, sampling temperature offers a direct and interpretable control knob for balancing
 136 exploration and exploitation in LLMs. Du *et al.* (Du et al., 2025) propose an adaptive inference-time
 137 method that selects optimal temperatures using multiple sampled generations. While effective for
 138 inference, it does not address how temperature can be dynamically optimized during RL training.
 139 Current LLM RL approaches either fix the temperature (Guo et al., 2025; Chen et al., 2025) or
 140 manually tune it (An et al., 2025; Liu et al., 2025), without incorporating trajectory feedback. Our
 141 work frames temperature as a learnable meta-policy that adapts exploration online, guided directly
 142 by trajectory advantages and likelihood to align LLM policy optimization.

143 **Meta-Policy in Reinforcement Learning.** Meta-policies have been studied in conventional RL. In
 144 hierarchical RL, the meta-policy acts as a high-level controller over low-level skills or options (Vezh-
 145 nevets et al., 2017; Bacon et al., 2017; Frans et al., 2017). MLSH (Frans et al., 2017) learns a set of
 146 reusable sub-policies, which are shared across tasks, while a task-specific master policy then com-
 147 poses these sub-policies to solve new tasks. Another line of work leverages meta-gradient methods
 148 to treat hyperparameters—such as discount factors, bootstrapping parameter λ —as differentiable
 149 variables updated through meta-gradients (Xu et al., 2018; Wang & Ni, 2020). Meta-SAC learns the
 150 optimal entropy regularization parameter in Soft Actor-Critic (Wang & Ni, 2020).

151 While these works highlight the potential of meta-policies in conventional RL, they have not been
 152 explored in the context of LLM RL. To the best of our knowledge, our approach is the first to treat
 153 sampling temperature as a meta-policy, directly addressing the exploration–exploitation trade-off
 154 during LLM RL. Note that the hyperparameters studied in (Xu et al., 2018; Wang & Ni, 2020)
 155 are differentiable, enabling direct optimization. In contrast, the sampling temperature in the typical
 156 LLM RL frameworks is non-differentiable, rendering these methods infeasible. We propose the
 157 practical TAMPO approach, which efficiently adapts the sampling temperature by reusing existing
 158 rollouts without requiring gradient-based optimization.

159

3 TEMPERATURE ADAPTIVE META POLICY OPTIMIZATION (TAMPO)

160 We aim to treat temperature as a learnable meta-policy that dynamically balances exploration and
 161 exploitation during LLM reinforcement learning. Given a discrete set of candidate temperatures

$\mathcal{T} = \{T_1, \dots, T_K\}$, we define a meta-policy $\pi(\mathcal{T})$ that outputs a probability distribution over temperatures. During training, each rollout is sampled at a temperature determined based on $\pi(\mathcal{T})$. To achieve this, we introduce Temperature Adaptive Meta-Policy Optimization (TAMPO), a hierarchical framework that shifts probability mass toward temperatures that produce high-advantage trajectories while suppressing ineffective ones.

In this section, we first review background in §3.1, then formalize the problem in §3.2, and finally present TAMPO in §3.3.

3.1 BACKGROUND

We consider an LLM parameterized by θ , trained with reinforcement learning. For a given prompt q , the model generates a trajectory $\tau_i = (o_{i,1}, \dots, o_{i,n})$ of n tokens, where each token $o_{i,t}$ is generated based on the state $s_{i,t} = (q, o_{i,<t})$. Reward is provided at the sequence level as r_i .

Critic-Free RL with GRPO. In LLM RL, critic-free algorithms have become widely adopted due to their scalability and simplicity. One representative method is Group Relative Policy Optimization (GRPO) (Shao et al., 2024; Guo et al., 2025), which provides a simple way to compute trajectory-level credit/advantage without an explicit critic. For a given prompt, it samples a group of G rollouts $\{\tau_1, \dots, \tau_G\}$ at a given temperature T . It then computes trajectory-level **advantages** A_i by normalizing rewards r_i within the group:

$$A_i = \frac{r_i - \text{mean}(\{r_1, \dots, r_G\})}{\text{std}(\{r_1, \dots, r_G\})}. \quad (1)$$

GRPO updates the policy $\pi_{\theta,T}$ by maximizing the expected advantage while including a KL regularization term with respect to a reference policy (see Appendix A for the full objective).

Temperature in Rollout Generation. During rollout generation, the sampling distribution is controlled by a temperature parameter $T > 0$, which scales the token logits $z(o_{i,t} \mid s_{i,t})$ as:

$$\pi_{\theta,T}(o_{i,t} \mid s_{i,t}) = \frac{\exp(z(o_{i,t} \mid s_{i,t})/T)}{\sum_{o'_{i,t}} \exp(z(o'_{i,t} \mid s_{i,t})/T)}. \quad (2)$$

The temperature controls the exploration–exploitation trade-off: too low results in over-exploitation, too high introduces excessive randomness, reducing useful exploration. Despite its importance, T is typically fixed, limiting policy optimization.

3.2 PROBLEM FORMULATION

We formalize temperature adaptation as a bilevel meta-optimization problem. The inner loop optimizes the LLM policy π_θ under temperatures sampled from the meta-policy π_ϕ , while the outer loop optimizes π_ϕ to maximize the performance of the LLM policy.

Let $\pi_\theta(\cdot \mid q; T)$ denote the model policy under temperature T (which we also denote as $\pi_{\theta,T}(\cdot \mid q)$), where $q \sim \mathcal{D}$ is a prompt. The meta-policy π_ϕ specifies a distribution over candidate temperatures. The inner objective is

$$\theta^*(\phi) = \arg \max_{\theta} \mathbb{E}_{q \sim \mathcal{D}} \mathbb{E}_{T \sim \pi_\phi} \mathbb{E}_{\tau \sim \pi_\theta(\cdot \mid q; T)} [r(\tau, q)], \quad (3)$$

while the outer objective seeks

$$\phi^* = \arg \max_{\phi} J_{\text{meta}}(\theta^*(\phi)), \quad (4)$$

where J_{meta} denotes the evaluation metric of interest (e.g., expected reward). This bilevel formulation highlights the adaptive role of temperature, but is not directly tractable in practice. Next, we describe our TAMPO.

3.3 TAMPO: MECHANISM AND IMPLEMENTATION

Tractability Challenge. In many LLM RL pipelines, rollout generation and policy optimization are typically decoupled: rollouts are generated using lower-precision models for efficiency, which

prevents backpropagation of gradients through the sampling process. This makes direct gradient-based optimization of the temperature meta-policy infeasible. Moreover, a naive trial-and-error strategy—generating rollouts for each candidate temperature—is computationally prohibitive. We thus seek a solution that works with the existing decoupled pipeline and requires no extra rollouts.

Key Observation. Every trajectory inherently encode its “preferred” temperature, *i.e.*, the temperature under which it is most likely to be generated (see Figure 2). Intuitively, for a high-reward (positive advantage) trajectory, we should reinforce temperatures that increase its likelihood; for a low-reward trajectory (negative advantage), we should down-weight such temperatures. *This insight provides a tractable signal for adapting temperature.*

Building on this idea, TAMPO treats temperature as a *learnable meta-policy* updated directly from trajectory-level signals. The meta-policy shifts probability mass toward temperatures associated with advantageous rollouts and suppresses ineffective ones, enabling adaptive exploration aligned with policy improvement.

3.3.1 TEMPERATURE-DEPENDENT TRAJECTORY LIKELIHOOD

The likelihood (i.e., probability) of a trajectory τ_i at temperature T from policy θ is

$$P_{\theta,T}(\tau_i) = \prod_{t=1}^{|\tau_i|} \pi_{\theta,T}(o_{i,t} | s_{i,t}). \quad (5)$$

To remove dependence on trajectory length, we use the **average log-likelihood** (likelihood for short hereafter):

$$\begin{aligned}\ell_T(\tau_i) &= \frac{1}{|\tau_i|} \log P_{\theta, T}(\tau_i) \\ &= \frac{1}{|\tau_i|} \sum_{t=1}^{|\tau_i|} \log \pi_{\theta, T}(o_{i, t} \mid s_{i, t}).\end{aligned}\quad (6)$$

We can probe the likelihoods of a trajectory τ_i under a set of **virtual temperatures** $T_k \in \mathcal{T}$ via (6). The trajectory likelihood is **unimodal** w.r.t. T (see the proof in Appendix B), and there exists a *likelihood-optimal temperature* T_i^* that maximizes the likelihood:

$$T^* = \arg \max_{T_k \in \mathcal{T}} \ell_{T_k}(\tau_i). \quad (7)$$

Figure 2 visualizes the trajectory likelihoods under different temperatures for 8 rollouts of a prompt, illustrating the unimodal nature. This implies that we can increase the likelihood of a trajectory by adjusting the temperature.

The empirical analysis in Appendix §C shows that positive advantage trajectories cluster to values T^* distinct from those of negative advantage trajectories, indicating that sampling from suitable temperatures can preferentially increase the likelihood of high advantage rollouts.

3.3.2 META-POLICY OPTIMIZATION WITH TEMPERATURE REWARDS

We formulate online temperature adaptation as a policy over temperature. A key challenge is evaluating the advantage of specific temperatures. Instead of sampling additional trajectories, we reuse the rollouts from inner-loop optimization. Particularly, for a trajectory with positive advantage, we increase its likelihood by rewarding temperatures that lead to higher trajectory likelihoods. Conversely, for a trajectory with negative advantage, we down-weight its likelihood by punishing temperatures that lead to higher trajectory likelihoods. This aligns temperature adaptation with policy optimization: reinforcing the likelihoods of high-reward trajectories, while suppressing likelihoods of low-reward trajectories.

Temperature-specific Advantage. Let τ_i denote a sampled trajectory and $\mathcal{T} = \{T_1, \dots, T_K\}$ a set of candidate temperatures. For each trajectory τ_i and virtual candidate temperature T_L , similar to

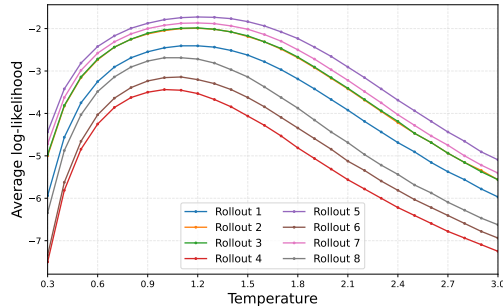


Figure 2: Example of trajectory likelihood under different temperatures for 8 rollouts of a prompt.

270 (6), we compute the trajectory's likelihood under the LLM policy θ at temperature T_k as
 271

$$272 \quad 273 \quad 274 \quad \ell_{T_k}(\tau_i) = \log P_{T_k}(\tau_i) = \sum_{t=1}^{|\tau_i|} \log \pi_{\theta, T_k}(o_{i,t} | s_{i,t}). \quad (8)$$

275 To capture the relative desirability of different temperatures, we normalize the likelihoods $\ell_{T_k}(\tau_i)$
 276 across the K candidate temperatures using *sparsemax* (Martins & Astudillo, 2016), yielding nor-
 277 malized likelihood $\hat{\ell}_{T_j}(\tau_i)$ with $\sum_{j=1}^K \hat{\ell}_{T_j}(\tau_i) = 1$. The trajectory's advantage A_i (see (1)) is then
 278 scaled by these normalized likelihoods to produce the *temperature-specific advantage*:

$$279 \quad 280 \quad 281 \quad \mathcal{A}_i^{(T_k)} = \hat{\ell}_{T_k}(\tau_i) \cdot A_i. \quad (9)$$

This can be interpretation as below:

- 282 • Positive-advantage trajectories ($A_i > 0$) reinforce the likelihood-optimal temperature most
 283 strongly, with neighboring temperatures receiving attenuated positive contributions.
- 284 • Negative-advantage trajectories ($A_i < 0$) penalize the likelihood-optimal temperature most, while
 285 nearby temperatures inherit attenuated negative contributions.

287 **Meta-policy Update.** Using trajectory's temperature-specific advantages, we maintain a meta-
 288 policy $\pi(T)$ over \mathcal{T} , which characterizes a probability distribution over \mathcal{T} . For a batch \mathcal{B} of $|\mathcal{B}|$
 289 samples, each with G generated trajectories, we aggregate the temperature-specific advantages for
 290 each candidate temperature T_k :

$$291 \quad 292 \quad 293 \quad \mathcal{A}_{\mathcal{B}}^{(T_k)} = \frac{1}{|\mathcal{B}|G} \sum_{b=1}^{|\mathcal{B}|} \sum_{i=1}^G \mathcal{A}_{b,i}^{(T_k)}, \quad (10)$$

294 where $\mathcal{A}_{b,i}^{(T_k)}$ denotes the temperature advantage of the i -th trajectory of sample b with respect to
 295 temperature T_k . $\mathcal{A}_{\mathcal{B}}^{(T_k)}$ serves as the update target for the meta-policy, representing the batch-level
 296 temperature-specific advantage.

297 To stabilize updates, we maintain an exponentially weighted moving average (EMA) of temperature-
 298 specific advantages:

$$300 \quad \bar{\mathcal{A}}_s^{(T_k)} = (1 - \alpha) \bar{\mathcal{A}}_{s-1}^{(T_k)} + \alpha \mathcal{A}_{\mathcal{B}}^{(T_k)}, \quad (11)$$

301 where $\alpha \in [0, 1]$ controls smoothing, s denotes training step index. This EMA provides a stabilized
 302 advantage estimate, reducing variance from individual batches while retaining responsiveness to
 303 new trajectory feedback.

304 Finally, the meta-policy $\pi_s(T_k)$ at step s is computed simply via min-max normalization:

$$306 \quad 307 \quad 308 \quad \pi_s(T_k) = \frac{\tilde{\mathcal{A}}_s^{(T_k)}}{\sum_{j=1}^K \tilde{\mathcal{A}}_s^{(T_j)}}, \quad \tilde{\mathcal{A}}_s^{(T_k)} = \frac{\bar{\mathcal{A}}_s^{(T_k)} - \min_j \bar{\mathcal{A}}_s^{(T_j)}}{\max_j \bar{\mathcal{A}}_s^{(T_j)} - \min_j \bar{\mathcal{A}}_s^{(T_j)}}, \quad k = 1, \dots, K. \quad (12)$$

309 This ensures $\pi_s(T_k)$ forms a valid distribution: $\sum_{k=1}^K \pi_s(T_k) = 1$, favouring higher-
 310 advantage temperatures while suppressing lower-advantage ones, and forming a valid distribution:
 311 $\sum_{k=1}^K \pi_s(T_k) = 1$.

312 3.4 OVERALL ALGORITHM

314 Algorithm 1 summarizes the TAMPO, which operates as a **hierarchical two-loop process**:

- 316 • **Inner loop:** Optimizes the LLM policy using trajectories (e.g., via GRPO) sampled under the
 317 temperature selected with meta-policy.
- 318 • **Outer loop:** Adaptively updates the temperature meta-policy. The same inner-loop trajectories are
 319 reused to update the meta-policy: trajectory advantages are modulated by their likelihoods under
 320 each candidate temperature as temperature-specific advantages (see Equations 8–9).

322 This **trajectory-guided update** enables principled online temperature adaptation, balancing explo-
 323 ration and exploitation **without extra rollouts**. TAMPO is compatible with critic-free RL algorithms
 and introduces negligible additional cost. We use GRPO as our critic-free RL in our experiments.

324 **Algorithm 1** Temperature Adaptive Meta Policy Optimization (TAMPO)

325

326 **Require:** LLM policy π_θ , reference policy π_{ref} , training step number S , temperature candidates

327 $\mathcal{T} = \{T_1, \dots, T_K\}$, temperature meta-policy π , EMA decay α .

328 1: Initialize $\bar{\mathcal{A}}_0^{(T_k)} \leftarrow 0$, $\pi_{s-1}(T_k) \leftarrow 1/K$ for all $T_k \in \mathcal{T}$.

329 2: **for** $s = 1$ to S **do**

330 3: **Outer Loop: Sample Temperature**

331 4: Sample temperature $T_s \sim \pi_{s-1}(T)$.

332 5:

333 6: **Inner Loop: Critic-free Policy Optimization**

334 7: Sample a batch of prompts \mathcal{B} .

335 8: **for** each prompt $q \in \mathcal{B}$ **do**

336 9: Generate G trajectories $\{\tau_1, \dots, \tau_G\}$ using π_θ at temperature T_s .

337 10: Compute reward $r(\tau_{q,i})$ and advantage $A_{q,i}$ (e.g., via GRPO) for each trajectory $\tau_{q,i}$.

338 11: Update LLM policy θ using advantages $A_{q,i}$.

339 12: **end for**

340 13:

341 14: **Outer Loop: Update Meta-Policy**

342 15: Calculate temperature-specific advantages $\mathcal{A}_\mathcal{B}^{(T_k)}$ for all $T_k \in \mathcal{T}$ (see (10)).

343 16: **for** each temperature $T_k \in \mathcal{T}$ **do**

344 17: Update EMA: $\bar{\mathcal{A}}_s^{(T_k)} \leftarrow (1 - \alpha) \bar{\mathcal{A}}_{s-1}^{(T_k)} + \alpha \mathcal{A}_\mathcal{B}^{(T_k)}$.

345 18: **end for**

346 19: Update meta-policy $\pi_s(T_k)$ based on the $\bar{\mathcal{A}}_s^{(T_k)}$ and (12) for all $T_k \in \mathcal{T}$.

347 20: **end for**

348 4 EXPERIMENTS

350 4.1 SETUP

352 **Training Datasets and Benchmarks.** We utilize a public math–reasoning dataset open-s1 (Dang
 353 & Ngo, 2025) for training. For evaluation, we use five distinct mathematics-focused benchmarks—**AIME24**, **MATH-500**, **AMC23**, **Minerva**, and **OlympiadBench**—covering a broad spec-
 354 trum of difficulty levels and problem styles to comprehensively assess reasoning ability and gen-
 355 eralization performance.

357 **Implementation Details.** We use DeepSeek-R1-Distill-Qwen-1.5B (DS-Qwen-1.5B for
 358 short) (Guo et al., 2025) as our base model to train both baselines and our models. We set our
 359 candidate temperatures in the range 0.6–1.5 with the interval 0.1, and $K = 10$, and the EMA
 360 coefficient $\alpha = 0.05$ by default. In the warmup phase (*i.e.*, the first 10% of training steps), we
 361 use a fixed sampling temperature of 1.0 for LLM policy, while the meta-policy is updated. After
 362 the warmup phase, the sampling temperature is determined dynamically by the online learned
 363 meta-policy. The maximum response length is set to 6k tokens.

364 All experiments are conducted on NVIDIA 8×V100 GPUs. We train both baseline models and our
 365 models for 200 steps, using an initial learning rate of 1×10^{-6} , a **warmup ratio of** 0.1, followed by
 366 a cosine schedule. The training batch size is set to 32, with 8 rollouts per question.

368 **Evaluation Protocol.** We evaluate using Pass@1 and Pass@8 in order to measure single-shot
 369 accuracy and performance under multiple sampled attempts, showing model’s exploration potential
 370 to solve questions. All evaluations are performed with a maximum response length of 6k tokens and
 371 a fixed decoding temperature of 1.0.

373 4.2 MAIN RESULTS

375 **Comparison with Baselines.** We adopt GRPO as the RL algorithm for both baselines and our
 376 scheme. DS-Qwen-1.5B refers to DeepSeek-R1-Distill-Qwen-1.5B, which serves as the starting
 377 model for all 1.5B model experiments. We construct baselines using a fixed sampling temperature
 at 0.9, 1.2, and 1.5 during training, denoted by GRPO ($T_s : 0.9$), GRPO ($T_s : 0.9$), and GRPO ($T_s :$

Method	Average		AIME24		MATH-500		AMC23		Minerva		OlympiadBench	
	Pass@1	Pass@8	Pass@1	Pass@8								
DS-Qwen-1.5B	39.1	57.8	13.3	26.7	76.2	89.2	45.0	72.5	22.8	41.5	38.4	59.0
GRPO ($T_s : 0.9$)	42.0	60.8	<u>20.0</u>	30.0	75.2	91.0	50.0	80.0	<u>26.1</u>	43.4	38.7	59.4
GRPO ($T_s : 1.2$)	41.6	61.1	<u>20.0</u>	33.3	<u>77.4</u>	90.6	50.0	<u>77.5</u>	22.4	43.4	38.1	60.5
GRPO ($T_s : 1.5$)	42.6	<u>62.1</u>	23.3	<u>36.7</u>	75.4	90.8	<u>52.5</u>	77.5	22.8	<u>44.5</u>	39.0	61.2
GRPO ($T_s : 0.9 \rightarrow 1.5$)	<u>42.8</u>	59.7	16.7	30.0	76.6	89.8	<u>55.0</u>	77.5	24.6	40.8	41.0	60.4
TAMPO (Ours)	44.5	63.8	23.3	40.0	<u>76.8</u>	91.0	55.0	82.5	27.9	44.8	<u>39.6</u>	<u>60.7</u>

Table 1: Comparison of TAMPO with baselines on math reasoning using 1.5B models, evaluated with Pass@1 and Pass@8. DS-Qwen-1.5B denotes DeepSeek-R1-Distill-Qwen-1.5B (Guo et al., 2025), which serves as the base model for all training on the open-s1 dataset. GRPO ($T_s : 0.9$) indicates a baseline trained with GRPO at a fixed sampling temperature of 0.9. The maximum response length is set to 6k tokens. The **best** performance is highlighted in bold and the second best is underlined.

0.9), respectively. Additionally, we include a baseline with a linearly increasing training temperature from 0.9 to 1.5, denoted as GRPO ($T_s : 0.9 \rightarrow 1.5$).

Table 1 reports Pass@1 and Pass@8 accuracy across the five evaluation benchmarks. On average, our TAMPO consistently outperforms the best fixed-temperature baseline, achieving 1.9% and 1.7% improvements in Pass@1 and Pass@8, respectively. Across all datasets, TAMPO either achieves the best performance or the second best, highlighting the effectiveness of treating temperature as a learnable meta-policy.

Complexity. Our scheme has nearly the same computational complexity compared to the baseline schemes. (i) The meta-policy model is extremely lightweight, as it only maintains a list of temperature advantages, introducing negligible overhead during training and being discarded at inference. (ii) TAMPO reuses rollouts from the inner loop, eliminating the need for generating additional trajectories. For the same number of training steps, both the baseline schemes using GRPO and our TAMPO use approximately the same training time (9 hours 54 minutes on an $8 \times$ V100 GPU machine for 200 steps).

4.3 ABLATION STUDY

Influence of EMA Coefficient α . As described in (11), α controls the exponential moving average smoothing, balancing the contribution of current feedback and historical accumulation. Table 2 reports the results for $\alpha \in \{0.01, 0.05, 0.10\}$. The increase in α from 0.01 to 0.05 increases the average score from 41.6 to 44.5 and all benchmarks showing improvement. Further increasing α to 0.10 produces mixed effects. $\alpha = 0.05$ provides a good trade-off between reducing variance and retaining responsiveness to new feedback.

α	Average	AIME24	MATH-500	AMC23	Minerva	OlympiadBench
0.01	41.6	20.0	75.2	50.0	<u>25.4</u>	37.5
0.05	44.5	23.3	76.8	<u>55.0</u>	27.9	39.6
0.10	<u>43.6</u>	<u>23.3</u>	<u>75.4</u>	57.5	23.2	<u>38.8</u>

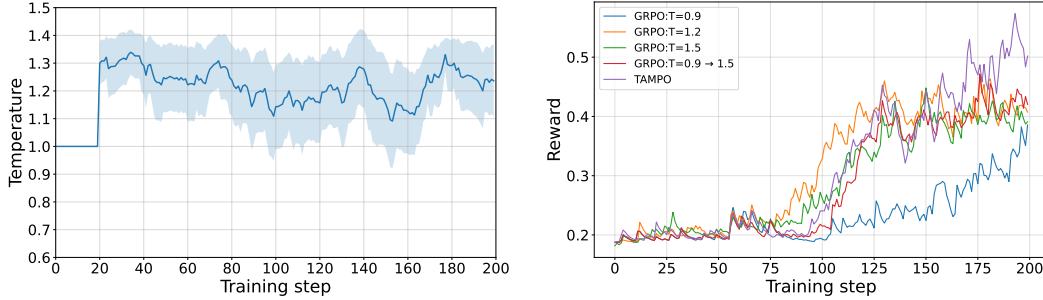
Table 2: Influence of the EMA coefficient α for our TAMPO. We report the performance on Pass@1.

Influence of Sampling Strategy on Meta-policy. We model the meta-policy as a distribution π over candidate temperatures. At each training step, similar to token sampling in LLM, we sample temperatures from π via nucleus sampling (*i.e.*, top-p sampling), which selects actions from the smallest set whose cumulative probability exceeds a threshold p , focusing on the “nucleus” of likely outcomes while filtering out low-probability options. p controls the trade-off between exploration and exploitation in the meta-policy.

Table 3 shows results for top-p sampling with $p = 0.9, 0.7, 0.5, 0$. When $p = 0$, this corresponds to greedy sampling, selecting the temperature with the highest probability (equivalent to top-k sampling with $k = 1$). We can see that a moderate threshold $p = 0.7$ achieves a good balance between exploration and exploitation on temperature. We set p to 0.7 by default. Too high a threshold lim-

	Sampling strategy	Average	AIME24	MATH-500	AMC23	Minerva	OlympiadBench
432	Top-p ($p: 0.9$)	43.0	20.0	76.6	52.5	26.1	39.7
433	Top-p ($p: 0.7$)	44.5	23.3	76.8	55.0	27.9	39.6
434	Top-p ($p: 0.5$)	42.2	23.3	75.4	50.0	24.3	38.1
435	Top-p ($p: 0$, greedy)	40.9	20.0	73.8	50.0	23.5	37.2
436							

Table 3: Influence of sampling strategy on meta-policy. We report the performance on Pass@1.



(a) Sampling temperatures from the meta-policy. (b) Reward curves for LLM policy models in training.

Figure 3: (a) Sampling temperatures from the meta-policy using nucleus sampling. (b) Rewarding curves of LLM policy models for baselines and our TAMPO.

its exploitation of the learned meta-policy, sacrificing certain opportunities to exploit the benefit of learned meta-policy. Too low a threshold (*e.g.*, $p = 0.5$) or greedy sampling (*i.e.*, $p = 0$) leads to under-exploration, reducing effectiveness. Since the greedy sampling always sample temperatures that having the highest advantages, even though the second-best temperature may have similar advantages, such under-exploration of temperatures leads to LLM policy losing opportunity to generate rollouts under those temperatures and reducing the experience diversity.

For the ablated schemes, we also show the reward curves for the LLM policy during training in Appendix §E. The schemes with the highest rewards also lead to the best performance on the evaluation benchmarks.

4.4 ANALYSIS

Sampling Temperature from Meta-policy. Figure 3 (a) visualizes the temperatures sampled from the meta-policy via nucleus sampling ($p = 0.7$). We report the mean and standard deviation over a sliding window of 25 training steps. We can see that the temperatures dynamically throughout training. After the 20 warm-up steps, a high temperature (around 1.3) is preferred, promoting stronger exploration in LLM policy generation. As training progresses, the mean temperature slightly decreases, favoring more exploitation while retaining sufficient diversity in rollouts.

Moreover, the observed fluctuations (large standard deviation) are due to nucleus sampling, which balances exploitation of the learned meta-policy with continued exploration, where the exploration on diverse temperatures enrich the trajectory patterns of the LLM policy.

Training Reward Curves. Figure 3 (b) shows the evolution of rewards during LLM policy training. Compared to baseline schemes (as shown in Table 1), TAMPO achieves the highest rewards as training goes, demonstrating that the adaptive temperature meta-policy effectively guides LLMs toward trajectories with greater expected returns.

5 CONCLUSION

We presented TAMPO, a hierarchical framework that treats temperature as a learnable meta-policy in LLM reinforcement learning. By reusing trajectories to adaptively update a temperature meta-policy, TAMPO enables exploration without extra rollouts and achieves consistent improvements on

486 mathematical reasoning benchmarks. These results demonstrate that principled temperature adapta-
 487 tion is a practical and effective tool for advancing LLM reinforcement learning.
 488

489 **LLM USAGE**

490 We used large language models (LLMs) to assist with refining the writing and presentation of this
 491 paper. LLMs were employed for improving clarity, conciseness, and formatting, while all ideas,
 492 methods, and experiments were conceived and executed by the authors.
 493

494 **REPRODUCIBILITY STATEMENT**

495 We have made extensive efforts to ensure the reproducibility of our work. Our temperature adap-
 496 tation method and algorithm are described in § 3.3. The training details, including base models,
 497 hyperparameters, and optimization settings, are described in § 4.1. The training datasets and eval-
 498 uation benchmarks used in this study are publicly available. We will release the source code upon
 499 acceptance to further facilitate the verification and reproduction of our results.
 500

501 **REFERENCES**

- 502 Chenxin An, Zhihui Xie, Xiaonan Li, Lei Li, Jun Zhang, Shansan Gong, Ming Zhong, Jingjing
 503 Xu, Xipeng Qiu, Mingxuan Wang, and Lingpeng Kong. Polaris: A post-training recipe for scal-
 504 ing reinforcement learning on advanced reasoning models, 2025. URL <https://hkunlp.github.io/blog/2025/Polaris>.
- 505 Pierre-Luc Bacon, Jean Harb, and Doina Precup. The option-critic architecture. In *Proceedings of
 506 the AAAI conference on artificial intelligence*, volume 31, 2017.
- 507 Yuntao Bai, Saurav Kadavath, Sandipan Kundu, Amanda Askell, Jackson Kernion, Andy Jones,
 508 Anna Chen, Anna Goldie, Azalia Mirhoseini, Cameron McKinnon, et al. Constitutional ai: Harm-
 509 lessness from ai feedback. *arXiv preprint arXiv:2212.08073*, 2022.
- 510 Qiguang Chen, Libo Qin, Jinhao Liu, Dengyun Peng, Jiannan Guan, Peng Wang, Mengkang Hu,
 511 Yuhang Zhou, Te Gao, and Wanxiang Che. Towards reasoning era: A survey of long chain-of-
 512 thought for reasoning large language models. *arXiv preprint arXiv:2503.09567*, 2025.
- 513 Quy-Anh Dang and Chris Ngo. Reinforcement learning for reasoning in small llms: What works
 514 and what doesn't. *arXiv preprint arXiv:2503.16219*, 2025.
- 515 Weihua Du, Yiming Yang, and Sean Welleck. Optimizing temperature for language models with
 516 multi-sample inference. *arXiv preprint arXiv:2502.05234*, 2025.
- 517 Kevin Frans, Jonathan Ho, Xi Chen, Pieter Abbeel, and John Schulman. Meta learning shared
 518 hierarchies. *arXiv preprint arXiv:1710.09767*, 2017.
- 519 Daya Guo, Dejian Yang, Haowei Zhang, Junxiao Song, Ruoyu Zhang, Runxin Xu, Qihao Zhu,
 520 Shirong Ma, Peiyi Wang, Xiao Bi, et al. Deepseek-R1: Incentivizing reasoning capability in llms
 521 via reinforcement learning. *arXiv preprint arXiv:2501.12948*, 2025.
- 522 Ari Holtzman, Jan Buys, Li Du, Maxwell Forbes, and Yejin Choi. The curious case of neural text
 523 degeneration. *arXiv preprint arXiv:1904.09751*, 2019.
- 524 Jian Hu, Jason Klein Liu, Haotian Xu, and Wei Shen. Reinforce++: An efficient rlhf algorithm with
 525 robustness to both prompt and reward models. *arXiv preprint arXiv:2501.03262*, 2025.
- 526 Leslie Pack Kaelbling, Michael L Littman, and Andrew W Moore. Reinforcement learning: A
 527 survey. *Journal of artificial intelligence research*, 4:237–285, 1996.
- 528 Wouter Kool, Herke van Hoof, and Max Welling. Buy 4 reinforce samples, get a baseline for free!
 529 In *International Conference on Learning Representations (ICLR) Workshop*, 2019.

- 540 Zihan Liu, Zhuolin Yang, Yang Chen, Chankyu Lee, Mohammad Shoeybi, Bryan Catanzaro, and
 541 Wei Ping. Acereason-nemotron 1.1: Advancing math and code reasoning through sft and rl
 542 synergy. *arXiv preprint arXiv:2506.13284*, 2025.
- 543 Andre Martins and Ramon Astudillo. From softmax to sparsemax: A sparse model of attention
 544 and multi-label classification. In *International conference on machine learning*, pp. 1614–1623.
 545 PMLR, 2016.
- 546 Long Ouyang, Jeffrey Wu, Xu Jiang, Diogo Almeida, Carroll Wainwright, Pamela Mishkin, Chong
 547 Zhang, Sandhini Agarwal, Katarina Slama, Alex Ray, et al. Training language models to fol-
 548 low instructions with human feedback. *Advances in neural information processing systems*, 35:
 549 27730–27744, 2022.
- 550 Deven Sethi, David Šiška, and Yufei Zhang. Entropy annealing for policy mirror descent in contin-
 551 uous time and space. *SIAM Journal on Control and Optimization*, 63(4):3006–3041, 2025.
- 552 Zhihong Shao, Peiyi Wang, Qihao Zhu, Runxin Xu, Junxiao Song, Xiao Bi, Haowei Zhang,
 553 Mingchuan Zhang, YK Li, Yang Wu, et al. Deepseekmath: Pushing the limits of mathemati-
 554 cal reasoning in open language models. *arXiv preprint arXiv:2402.03300*, 2024.
- 555 Han Shen. On entropy control in llm-rl algorithms. *arXiv preprint arXiv:2509.03493*, 2025.
- 556 Richard S Sutton, Andrew G Barto, et al. *Reinforcement learning: An introduction*, volume 1. MIT
 557 press Cambridge, 1998.
- 558 Alexander Sasha Vezhnevets, Simon Osindero, Tom Schaul, Nicolas Heess, Max Jaderberg, David
 559 Silver, and Koray Kavukcuoglu. Feudal networks for hierarchical reinforcement learning. In
 560 *International conference on machine learning*, pp. 3540–3549. PMLR, 2017.
- 561 Da Wang, Wei Wei, Lin Li, Xin Wang, and Jiye Liang. Rethinking exploration-exploitation trade-off
 562 in reinforcement learning via cognitive consistency. *Neural Networks*, 187, 2025.
- 563 Yufei Wang and Tianwei Ni. Meta-sac: Auto-tune the entropy temperature of soft actor-critic via
 564 metagradient. *arXiv preprint arXiv:2007.01932*, 2020.
- 565 Wikipedia contributors. Exploration-exploitation dilemma, 2025. URL https://en.wikipedia.org/wiki/Exploration%20vs%3Dexploitation_dilemma. Ac-
 566 cessed: 2025-08-18.
- 567 Zhongwen Xu, Hado P van Hasselt, and David Silver. Meta-gradient reinforcement learning. *Ad-
 568 vances in neural information processing systems*, 31, 2018.
- 569 Qiying Yu, Zheng Zhang, Ruofei Zhu, Yufeng Yuan, Xiaochen Zuo, Yu Yue, Weinan Dai, Tiantian
 570 Fan, Gaohong Liu, Lingjun Liu, et al. DAPO: An open-source llm reinforcement learning system
 571 at scale. *arXiv preprint arXiv:2503.14476*, 2025.
- 572 Daniel M Ziegler, Nisan Stiennon, Jeffrey Wu, Tom B Brown, Alec Radford, Dario Amodei, Paul
 573 Christiano, and Geoffrey Irving. Fine-tuning language models from human preferences. *arXiv
 574 preprint arXiv:1909.08593*, 2019.
- 575

583 A GRPO OPTIMIZATION OBJECTIVE

584 GRPO updates the policy $\pi_{\theta, T}$ by maximizing the expected advantage while including a KL regu-
 585 larization term with respect to a reference policy:

$$586 \mathcal{J}_{\text{GRPO}}(\theta) = \mathbb{E}_{(q, a) \sim \mathcal{D}, \{\tau_i\}_{i=1}^G \sim \pi_{\theta_{\text{old}}, T}} (\cdot | q) \\ 587 \left[\frac{1}{G} \sum_{i=1}^G \frac{1}{|\tau_i|} \sum_{t=1}^{|\tau_i|} \left((\rho_{i,t}(\theta, T) A_i, \text{clip}(\rho_{i,t}(\theta, T), 1 - \epsilon, 1 + \epsilon) A_i) - \beta D_{\text{KL}}(\pi_{\theta, T} || \pi_{\text{ref}}) \right) \right], \\ 588 \quad (13)$$

589 where $\rho_{i,t}(\theta, T) = \frac{\pi_{\theta, T}(o_{i,t} | q, o_{i, < t})}{\pi_{\theta_{\text{old}}, T}(o_{i,t} | q, o_{i, < t})}$. ϵ and β are hyperparameters.

594 B PROOF OF THE UNIMODAL OF TRAJECTORY LIKELIHOOD W.R.T. T
595

596 For a trajectory $\tau = (a_1, \dots, a_n)$ of n tokens, each token a_t is generated based on the state
597 $s_t = (q, a_{<t})$ with policy model parameterized by θ . Here q denotes the prompt/question. Under
598 temperature scaling of $T > 0$, the conditional distribution can be obtained based on the model
599 output logits $z(a | s_t)$ as

$$600 \pi_{\theta, T}(a | s_t) = \frac{\exp(z(a | s_t)/T)}{\sum_{a'} \exp(z(a' | s_t)/T)}. \quad (14)$$

603 The log-likelihood of the trajectory $\tau = (a_1, a_2, \dots, a_n)$ is

$$605 \ell_T(\tau) = \log P_{\theta, T}(\tau), \quad \text{where } P_{\theta, T}(\tau) = \prod_{t=1}^n \pi_{\theta, T}(a_t | s_t). \quad (15)$$

608 We define a baseline distribution at $T=1$ under condition s_t as¹

$$610 q_t(a) := \frac{e^{z(a | s_t)}}{\sum_u e^{z(u | s_t)}}. \quad (16)$$

612 Then,

$$613 \log q_t(a) = z(a | s_t) - \log \sum_u e^{z(u | s_t)}. \quad (17)$$

615 Let $\beta = 1/T$ which denotes the inverse temperature. We have

$$617 \pi_{\theta, T}(a | s_t) = \frac{q_t(a)^\beta}{\sum_u q_t(u)^\beta}. \quad (18)$$

619 Let us define $S(\tau) := \sum_{t=1}^n \log q_t(a_t)$, $A_t(\beta) := \log \sum_u q_t(u)^\beta$, and $A(\beta) := \sum_{t=1}^n A_t(\beta)$. We
620 obtain the standard exponential family form:

$$621 \log P_{\theta, \beta}(\tau) = \beta S(\tau) - A(\beta). \quad (19)$$

623 **Second derivative w.r.t the inverse temperature β (unimodality):** Based on standard properties,

$$625 A'_t(\beta) = \mathbb{E}_{a \sim \pi_{\theta, T}(\cdot | s_t)} [\log q_t(a)], \quad A''_t(\beta) = \text{Var}_{a \sim \pi_{\theta, T}(\cdot | s_t)} [\log q_t(a)] \geq 0. \quad (20)$$

626 Then,

$$627 \frac{d^2}{d\beta^2} \log P_{\theta, \beta}(\tau) = -A''(\beta) \leq 0. \quad (21)$$

629 Therefore, $\log P_{\theta, \beta}(\tau)$ is strictly concave in β . Since $\beta = 1/T$ is a monotone reparameterization,
630 $P_{\theta, T}(\tau)$ is unimodal in T , with a one-to-one correspondence between maximizers: $\beta^*(\tau) = 1/T^*(\tau)$.

632 **First derivative w.r.t. temperature and endpoint limits (typical “rise-then-fall”):** We have

$$634 \log \pi_{\theta, T}(a | s_t) = \frac{z(a | s_t)}{T} - \log \sum_u \exp(z(u | s_t)/T). \quad (22)$$

636 Let us define $\mu_T(s_t) := \mathbb{E}_{a \sim \pi_{\theta, T}(\cdot | s_t)} [z(a | s_t)]$. A direct differentiation yields

$$638 \frac{d}{dT} \log \pi_{\theta, T}(a | s_t) = -\frac{1}{T^2} [z(a | s_t) - \mu_T(s_t)]. \quad (23)$$

640 Therefore,

$$641 \ell'_T(T) = \frac{d}{dT} \log P_{\theta, T}(\tau) = -\frac{1}{T^2} \sum_{t=1}^n [z(a | s_t) - \mu_T(s_t)]. \quad (24)$$

644 As $T \rightarrow 0^+$, each step tends to select the action with maximum logit. Therefore, $\mu_T(s_t) \rightarrow$
645 $\max_a z(a | s_t)$. When the trajectory is not composed by greedy sampling of actions/tokens,
646 $z(a | s_t) < \mu_T(s_t)$ and then $\ell'_T(T) > 0$, i.e., a small increase of T increases $\log P_{\theta, T}(\tau)$.

647 ¹We denote $q_t(a_t | s_t)$ by $q_t(a_t)$ for conciseness.

648 As $T \rightarrow \infty$, $\pi_{\theta, T}$ approaches uniform distribution and $\mu_T(s_t) \rightarrow \bar{z}(s_t) = |\mathcal{V}|^{-1} \sum_a z(a \mid s_t)$. The
 649 LLM sampled tokens in general have $z(a \mid s_t) > \bar{z}(s_t)$ (except for an edge case), making the sum
 650 positive and $\ell'_T(T) < 0$, *i.e.*, a increase of T reduces $\log P_{\theta, T}(\tau)$.
 651

652 **Conclusion: unimodality and “rise-then-fall”.** Combining the strict concavity w.r.t. β (Eq. (21))
 653 and the opposite signs of $\ell'_T(T)$ at the low- and high-temperature limits (Eq. 24), we conclude that,
 654 for trajectories except edge cases, there exists a unique $T^*(\tau) \in (0, \infty)$ such that
 655

$$\ell'_T(T) > 0 \text{ for } T < T^*, \quad \ell'_T(T^*) = 0, \quad \text{and } \ell'_T(T) < 0 \text{ for } T > T^*. \quad (25)$$

656 Log-likelihood $\log P_{\theta, T}(\tau)$ is *typically* unimodal w.r.t T and exhibits a “rise-then-fall” shape beside
 657 edge cases.
 658

659 **Edge cases.** First, if a trajectory is composed of greedy tokens, that is, at every step t LLM policy
 660 picks the most probable token, then its likelihood decreases monotonically with T , approaching 1
 661 as $T \rightarrow 0^+$. Second, if a trajectory has many chosen tokens having probability below $|\mathcal{V}|^{-1}$, *i.e.*,
 662 which rarely occur under the decoding strategy, its likelihood will slowly increase when T increases.
 663

664 The unimodal property of the trajectory log-likelihood for general cases, and the monotonicity for
 665 edge cases, all assure that we can use discrete temperatures (as virtual temperatures) to well estimate
 666 the likelihood of trajectories under different temperatures.
 667

667 C CONNECTION BETWEEN TEMPERATURE AND ADVANTAGE

669 To gain a more intuitive understanding of the correlation between trajectory advantage and
 670 likelihood-optimal temperature, we conducted training under fixed sampling temperatures (0.9, 1.2,
 671 and 1.5) using GRPO and computed the likelihood-optimal temperature $T^*(\tau)$ for each trajectory
 672 τ . Figure 4 shows the resulting distributions for trajectories with positive advantages (green) and
 673 negative advantages (red) along training, with mean and variance computed for rollouts of every 5
 674 training steps.
 675

676 Three patterns can be observed. (i) A fixed sampling temperature generally does not align with the
 677 likelihood-optimal temperatures observed during training. (ii) Positive-advantage trajectories cluster
 678 around distinct T^* values compared to negative-advantage trajectories, indicating that high-reward
 679 rollouts are intrinsically associated with specific temperature regimes. (iii) At extreme sampling
 680 temperatures, trajectories tend to revert toward moderate T^* values: when $T = 1.5$, most T^* are
 681 well below 1.5, while at $T = 0.9$, most T^* are well above 0.9. This demonstrates that both excessive
 682 randomness and excessive determinism reduce the likelihood of producing advantageous rollouts.
 683

684 Overall, these results suggest that there exist more optimal temperatures that increase the proba-
 685 bility of high-advantage trajectories, highlighting substantial room for improving the likelihood of
 686 sampling advantageous rollouts.
 687

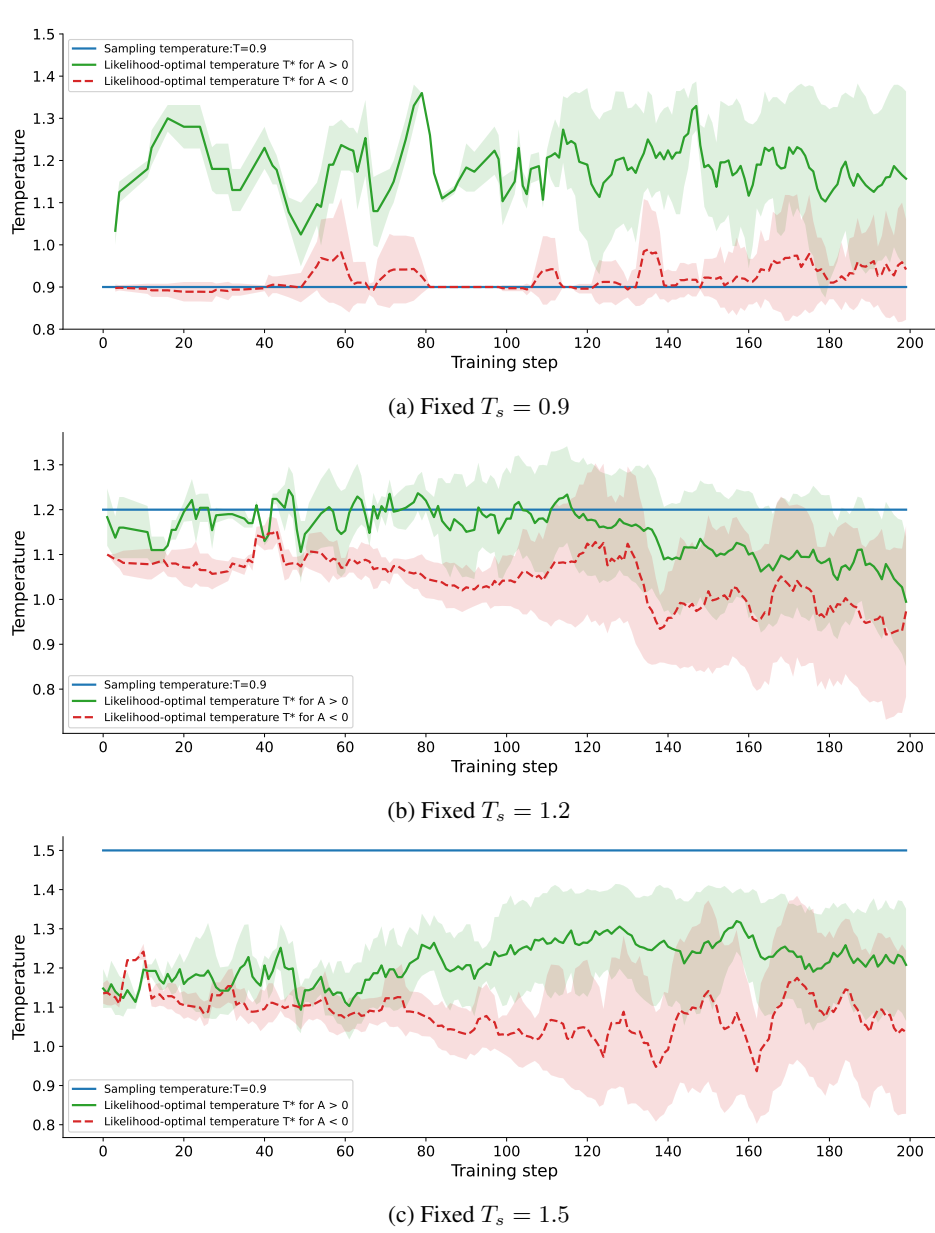
686 D MORE REWARD CURVES

688 We show the reward curves for the LLM policy during training for the ablated schemes. The schemes
 689 with the highest rewards also lead to the best performance on the evaluation benchmarks (see Fig-
 690 ure 5 and Figure 6).
 691

692 E MORE EXPERIMENTS RESULTS

694 To assess the stability of our method under different random seeds, we conducted three independent
 695 training runs of TAMPO. Table 4 reports the complete results of Pass@1 and Pass@8 across all
 696 mathematical reasoning benchmarks. As shown, performance across seeds remains highly consis-
 697 tent, demonstrating that TAMPO exhibits stable optimization dynamics and effective performance.
 698

699 To evaluate TAMPO’s generality across different base models and domains, we conducted addi-
 700 tional experiments. Specifically, we used Qwen2.5-3B-Instruct as a new base model and evaluated
 701 TAMPO on ECQA, a commonsense reasoning benchmark. The results in table 5, show consistent
 702 improvements, demonstrating that TAMPO generalizes beyond mathematical reasoning.
 703

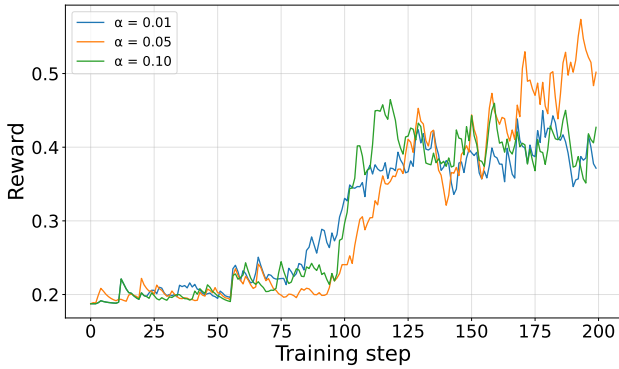
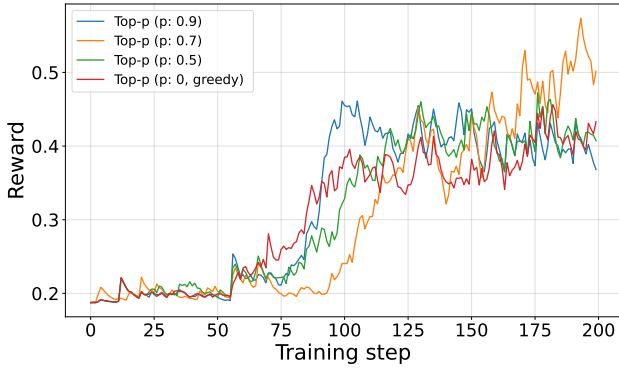


742
743
744
745
746
747
748
749
750
751
752
753
754
755

Figure 4: Distribution of trajectory likelihood-optimal temperatures under three fixed training temperatures, respectively. Green curve corresponds to the likelihood-optimal temperatures of positive-advantage trajectories ($A > 0$), red curve to negative-advantage trajectories ($A < 0$), and blue curve to the sampled fixed temperature.

Method	Average		AIME24		MATH-500		AMC23		Minerva		OlympiadBench	
	Pass@1	Pass@8	Pass@1	Pass@8	Pass@1	Pass@8	Pass@1	Pass@8	Pass@1	Pass@8	Pass@1	Pass@8
TAMPO (Ours) Run 1	44.5	63.8	23.3	40.0	76.8	91.0	55.0	82.5	27.9	44.8	39.6	60.7
TAMPO (Ours) Run 2	44.6	63.6	20.0	36.7	77.6	90.8	57.5	85.0	28.7	45.6	39.2	59.9
TAMPO (Ours) Run 3	44.3	63.6	23.3	40.0	76.6	90.8	55.0	82.5	26.8	44.5	39.9	60.4

Table 4: Three independent runs of TAMPO on math reasoning benchmarks (Pass@1 and Pass@8).

Figure 5: Reward curves for LLM policy models when using different EMA coefficient α values.Figure 6: Reward curves for LLM policy models under different p values for top-p sampling of meta-policy.

Method	Pass@1	Pass@8
Qwen2.5-3B-Instruct (no RL)	73.06%	77.76%
GRPO	75.07%	78.94%
TAMPO	76.12%	79.67%

Table 5: ECQA results evaluated with Pass@1 and Pass@8.